Global and Local Mesh Morphing
for Complex Biological Objects from µCT Data

D. Knötel[1,3], C. Becker[2,3], G. Scholtz[2,3] and D. Baum[1,3]

[1]Zuse Institute Berlin, Germany
[2]Humboldt-Universität zu Berlin, Institut für Biologie, Germany
[3]Cluster of Excellence Image Knowledge Gestaltung, Berlin, Germany

Abstract

We show how biologically coherent mesh models of animals can be created from µCT data to generate artificial yet naturally looking intermediate objects. The whole pipeline of processing algorithms is presented, starting from generating topologically equivalent surface meshes, followed by solving the correspondence problem, and, finally, creating a surface morphing. In this pipeline, we address all the challenges that are due to dealing with complex biological, non-isometric objects. For biological objects it is often particularly important to obtain deformations that look as realistic as possible. In addition, spatially non-uniform shape morphings that only change one part of the surface and keep the rest as stable as possible are of interest for evolutionary studies, since functional modules often change independently from one another. We use Poisson interpolation for this purpose and show that it is well suited to generate both global and local shape deformations.

CCS Concepts

•*Computing methodologies* → *Image processing; Mesh models;* Shape analysis; •*Applied computing* → Imaging;

1. Introduction

Over the past decade, access to image acquisition facilities offering techniques like computed tomography has become much easier. This enables the visualization of biological objects and structures for a wide range of scientific applications. As a result, biologists as well as researchers from other research areas working with biological objects can refer to realistic virtual representations of real biological data. This leads to a growing need of data processing solutions for such data, including image segmentation, model generation, and shape analysis.

In this paper, we show how to create biologically coherent animal models from µCT data and how these models can be interpolated in a naturally looking way using Poisson interpolation. We present the whole pipeline of processing algorithms, starting from generating topologically equivalent but still realistically looking surface triangle meshes from complex biological, non-isometric objects, then solving the correspondence problem, and finally, creating a surface morphing with naturally looking intermediate surfaces. In addition to global deformations, spatially non-uniform shape morphings that only change one part of the surface and keep the rest as stable as possible are of great interest. Here, we present all computational steps in order to allow other scientists from the application area to reproduce our findings.

As input data we use µCT scans of a lobster-like animal and a crab. The processing of these two datasets leads to non-isometric surface representations, e.g. due to differently sized tails, a folded tail (crab) versus an unfolded tail (lobster), and due to different scissor positions. On the other hand, both datasets exhibit enough similarities like the number of legs or the number of tail segments to allow a mapping of all parts of the two animals. This project was carried out as a collaboration between biologists, psychologists and computer scientists. The project was motivated by the psychologists who until now have been using very simple two-dimensional artificial intermediate images between lobster and crab for their experiments (see Reindl et al. [RSB*15]) in order to study the adaptation effect [CSL*07]. The results of our work will allow them to use far more realistic three-dimensional models as their experimental data that much better resemble real crabs and lobsters even though being artificial. Our collaborators are convinced that these models will be much better suited for their psychological studies, introducing less artifacts and thus less bias to their experiments. To date, the experiments, in which test persons have to rate the closeness of modified (interpolated) images to the original images, have not been carried out.

2. Related work

To the best of our knowledge, there are no papers working on similar complex biological data and performing all steps from CT data to shape morphing. Our workflow consists of three steps: (i) seg-

mentation and surface generation step; (ii) the creation of a one-to-one surface correspondence; and (iii) (local) shape morphing. Creation of surface mesh correspondence has attracted a lot of attention in previous years. For an overview see the survey by van Kaick et al. [vKZHCO11]. Main techniques are cross-parametrization methods, where the inputs are parametrized to simpler domains (e.g. Kraevoy et al. [KS04]), non-rigid registration methods, or methods based on the Heat Kernel Map [OMMG10] or the generalized multidimensional scaling (GMDS) approach by Bronstein et al. [BBK06]. For shape morphing, we are only interested in surface- and mesh-based methods. An overview about variational methods can be found in the survey by Botsch et al. [BS08].

3. Data

We used the stone crab *Xantho poressa* as our crab dataset and the Japanese crayfish *Cambaroides japonicus* as our "lobster" dataset. As a crayfish, *C. japonicus* is not a proper lobster but it is closely related to lobsters and looks very similar while being much smaller. This allowed us to use the same high-resolution µCT scanner for both animals. The µCT scans were conducted at Museum für Naturkunde Berlin (Germany) using a Phoenix nanotom X-ray|s tube at 50 kV and 200 µA, generating 1440 projections per scan over a 360° sample rotation. The cone beam reconstruction was performed using the datos|x-reconstruction software (GE Sensing & Inspection Technologies GMBH phoenix|x-ray) and a stack of virtual sections was produced and exported with VGStudio Max (Volume Graphics, Heidelberg). The datasets were resampled from a voxel size of 12.22 µm to a voxel size of 24.44 µm to reduce the size of the images and speed up processing.

If not stated otherwise, computations used in our workflow were carried out in the visualization software Amira ZIB Edition, which is an extension of Amira [SWH05].

4. Generation of closed manifold surfaces

The two original µCT images were segmented using a combination of thresholding and manual segmentation. This did not lead to a closed surface because not all structures, e.g. soft tissue, are visible in a CT scan, see Figure 1 (a). Therefore, we used additional methods to fill these gaps: (i) thresholding on an ambient occlusion computation [BT16] to close gaps in the legs; (ii) Poisson reconstruction [KH13] for closing the lobster carapace (upper shell) using Meshlab [CCC*08], and (iii) a convex hull computation for closing the crab carapace (see Figure 1). These intermediate results were corrected by shrinkage, growth and manual operations and finally combined into one segmentation, which was smoothed in order to create a closed watertight manifold surface. The final results can be seen in Figure 2. The meshes were resampled from approximately 3.3 M vertices to approximately 500,000 vertices using the remeshing algorithm by Zilske et al. [ZLZ08], implemented in Amira.

5. Solving the correspondence problem

We followed the workflow by Zöckler et al. [ZSH00] to create correspondence between the surface meshes. To this end, we subdivided the surfaces into smaller patches that are homeomorphic to a disk. We manually drew paths on the meshes leading to 142

different patches on both surfaces. These patches were created in agreement with the participating crustaceologists to ensure as high correctness as possible. In Figure 2, the patches are depicted by pseudo-coloring the surface meshes. We used this manual approach instead of more recent and automated solutions to get as much control as possible and to easily handle problems with non-isometric data. Since we are only working with two datasets, this additional time commitment is feasible and enabled us to include the knowledge of crustaceologists. For solving the final correspondence problem, each patch was mapped to the unit disk using mean-value parametrization [FH05], which finally leads to a one-to-one correspondence between the surfaces.

6. Mesh interpolation

Rotations, such as the tail movement of our datasets, cannot be described by linear interpolation, see for example our discussion section or the section about shape shrinkage in the Poisson interpolation paper by Xu et al. [XZWB06]. Therefore, we apply Poisson interpolation, which circumvents the problem resulting in rotations. Additionally, it allows local shape interpolation.

We shortly introduce the theory behind Poisson interpolation; for more details see the original paper. Source mesh and target mesh are stored as mesh scalar functions on the vertices of the domain mesh for their x, y and z coordinates, respectively. For these mesh scalar functions, the discrete gradient is computed on the domain mesh triangles. The gradients of source mesh and target mesh are interpolated and the discrete divergence of the interpolated gradients is computed. Solving the discrete Poisson equation leads back to mesh scalar functions and the interpolated mesh result (translation can be set arbitrarily). The gradient interpolation is done in the following non-linear way: For two corresponding triangles, the unique transformation matrix H is computed and decomposed via polar decomposition into a rotation matrix R and a symmetric, positive definite matrix S such that $H = RS$. The interpolation matrix H_t is computed by $H_t = R_t((1-t)I + tS)$, where t is the time parameter, R_t is the rotation matrix obtained by linearly interpolating the rotation angle of R, and I is the identity matrix. The transformation H_t is applied to the source gradient fields, which leads to the interpolated gradients. Local shape interpolation can be directly included into the computation of H_t. In this case the simple time parameter t is replaced by a parameter that depends on the time step and on the specific triangle. Some triangles are fully interpolated, some partially and some not at all.

We used the lobster mesh as the domain mesh. Especially for the tail triangles, we interpolated the rotation angle from 0 up to the angle value (of R), independent of the shortest interpolation direction (if the angle is larger than π). The linear system for the Poisson problem was solved with a direct sparse LLT Cholesky factorization with the Eigen [GJ*10] library. The Cholesky decomposition is only computed once in a preprocessing step. We used mesh distance fields to control local deformations. For example, to transform the tail and keep the rest of the mesh as stable as possible, we computed the distances of the mesh triangles to the tail region. Triangles belonging to the tail are fully interpolated, triangles near the tail partially and the rest of the triangles is not interpolated at all. Final morphing results using local as well as global interpolations can be seen in Figure 3.
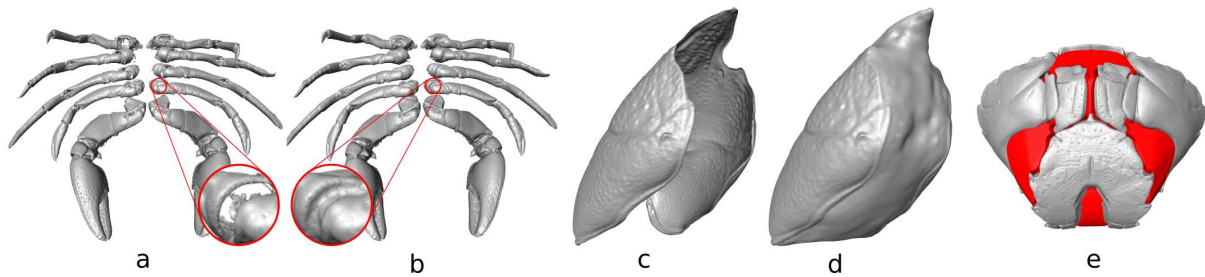
Figure 1: *Generation of closed manifold surfaces. a) Parts of the lobster legs segmented from the µCT scan. b) Gaps in the legs are closed using the segmentation of an ambient occlusion field. c) Part of the lobster carapace segmented from the µCT scan. d) Closing of the carapace as a result of Poisson reconstruction. e) In gray: parts of the crab carapace segmented from the µCT scan. In red: areas generated by computing the convex hull of the gray parts.*
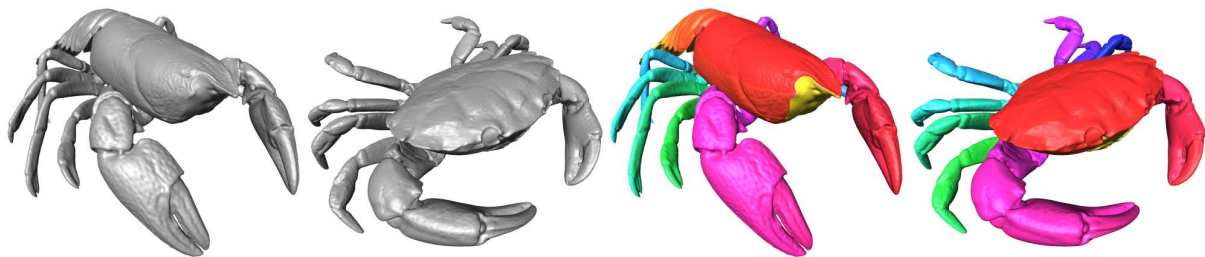

Figure 2: *From left to right: Lobster surface, crab surface, lobster surface with 142 patches, crab surface with 142 patches. In the two right-most images, the patch ids have been mapped to the surfaces using pseudo-colors.*
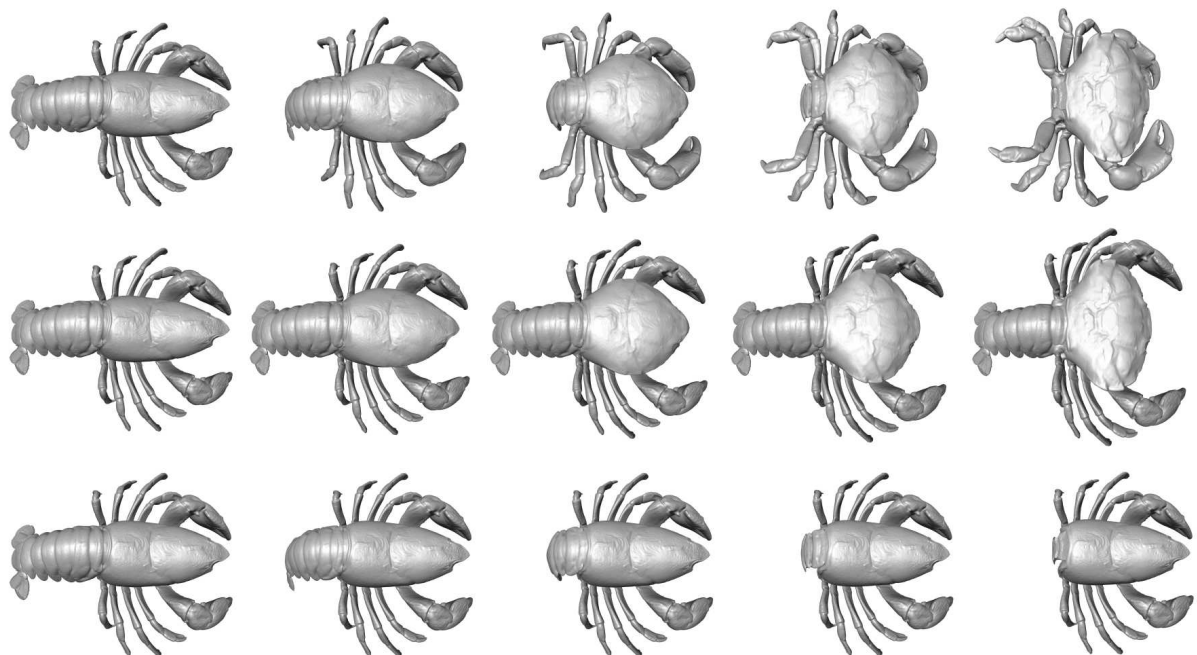

Figure 3: *Our interpolation results. From left to right: Interpolation from lobster to crab with time parameters 0.0, 0.25, 0.5, 0.75, 1.0. First row: Interpolation of the whole surface mesh (global morphing). Second row: Interpolation of the carapace only (local morphing). Third row: Interpolation of the tail only (local morphing).*
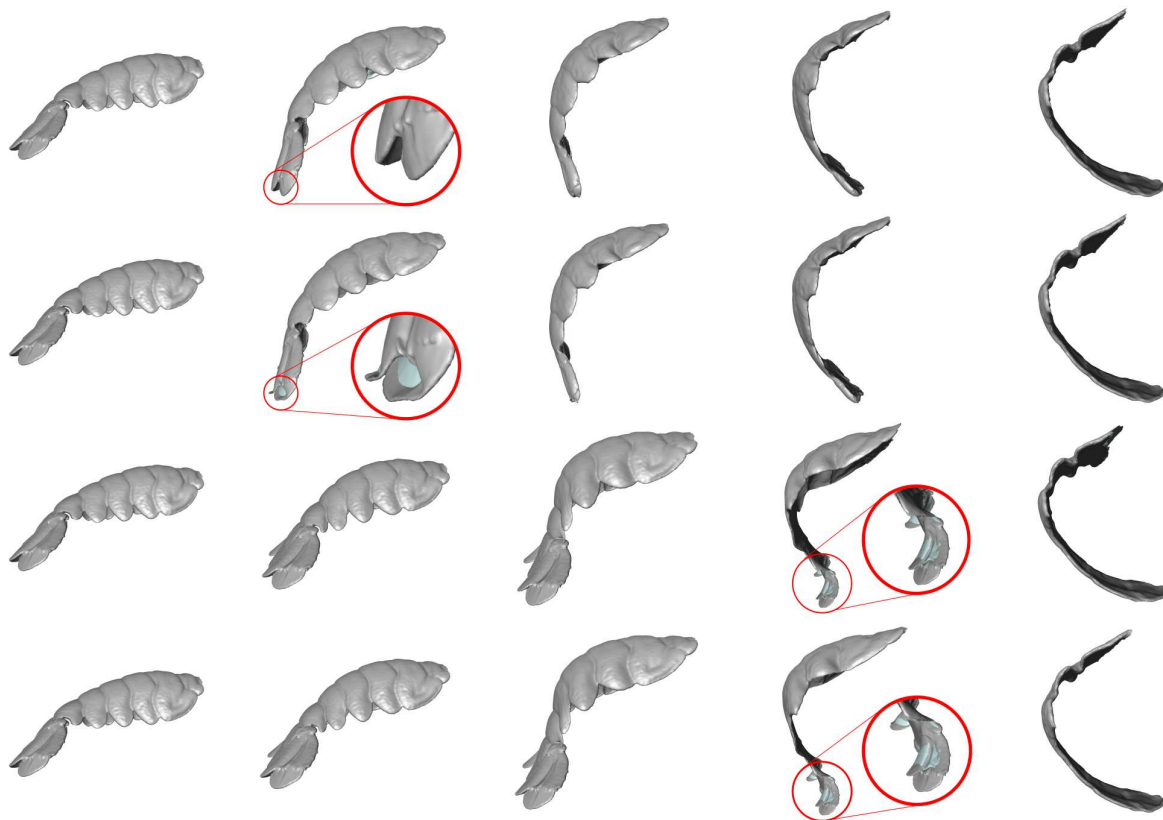
Figure 4: *Interpolation of the tail. From left to right: Interpolation from lobster tail to crab tail with time parameters 0.0, 0.25, 0.5, 0.75, 1.0. First row: Our interpolation result, that is, Poisson interpolation with special angle interpolation for the tail. Second row: Poisson interpolation with standard angle interpolation. Third row: Interpolation proposed by Alexa [Ale03]. Fourth row: Simple linear interpolation.*

7. Discussion & Conclusion

We successfully created realistic high-resolution surface models from µCT scans of a crab and a lobster-like dataset and used them to perform a naturally looking local mesh morphing. Videos of the morphings can be found in the supplementary material.

7.1. Surface model generation and correspondence

During the initial surface generation, we had to fill holes in the parts that had been segmented from the µCT scans. Since these holes were due to the usage of µCT, one possibility to circumvent this step would be to use additional scanning technologies, e.g. MRT scans, where previously hidden structures become visible. However, such a multi-modal imaging approach is expensive. On the other hand, it is still unlikely that with this approach all gaps will be closed. Therefore, we used a more artistic approach and applied supporting algorithms in combination with manual corrections. This lead to a high degree of freedom, which also allowed us to integrate the knowledge of the crustaceologists.

The creation of the surface model took several days for each animal. However, we do not see an easy way to circumvent this manual labor. Once the surface models had an equivalent topology, we used surface patchification to solve the correspondence problem. This worked well but also required a lot of manual labor, which was feasible in our application because we only investigated two datasets. If considerably more datasets need to be processed, this step clearly needs speeding up. This might be possible with semi-automatic methods as those mentioned in the related work but will definitely remain a challenge given the complexity of the investigated objects.

7.2. Mesh interpolation

For the tail, we interpolated the angles from 0 up to the angle of the rotation matrix of the polar decomposition, instead of taking the direction of the shortest angle interpolation. This was necessary because of the large angle difference for the tail triangles, which is due to the unfolded tail of the lobster and the folded tail of the crab. The first two rows of Figure 4 compare the two angle interpolation schemes and highlight the need for this special treatment.

Additionally, in rows three and four of Figure 4, we show the problems of linear algorithms when dealing with rotations, irrespective of whether it is linear interpolation on differential coordinates [Ale03], which would allow local mesh deformation, or simple linear interpolation on global vertex coordinates. As our

results clearly show, Poisson interpolation is very well suited for our purposes. We did not observe any problems with this interpolation method despite the large number of triangles and the great complexity of the animal morphologies. However, if the angle interpolation problem could be solved automatically, this would even further improve the applicability of this method.

7.3. Applications

The proposed pipeline was developed to support psychological studies investigating the adaptation effect [CSL*07], which has been well studied for human faces. The aim of this project was to investigate how far the results from the studies of human faces would translate to other objects. Here, for the first time, biological objects were used for such experiments. As a first approach, 2D morphing techniques were used, which resulted in rather poor representations of intermediate objects [RSB*15]. Using the generated models and the proposed interpolation method presented here, our collaborating psychologists are now able to generate all images required for this study. They are fully satisfied with the quality of the images and consider them as being perfectly suited for their studies. Of particular importance was the ability of creating local morphings that allow one to investigate the influence of one particular part of the object on the classification result. In order to reduce biases, the biologists among the authors insisted on intermediate objects that, even though being artificial, would still look natural. This was not the case for linear interpolations but only for the Poisson interpolation.

8. Future Work

The next step is to carry out the psychological experiments with the images created using our processing pipeline and compare the results with those obtained using the 2D morphings. Additionally, since we now have 3D morphed objects, a further series of experiments could be carried out using VR techniques in combination with eye tracking. This might allow the psychologists to understand which parts of the objects influences the classification results.

Even though the main motivation of our work was to carry out psychological experiments, the crab and lobster models can also be used for biometric research or as hypothetical evolutionary models. For example, it would be interesting to adjust the models to existing intermediate individuals using natural species, which have a body form intermediate between a lobster and a crab (e.g. porcellanid crabs). For this, different parts of the models would have to be morphed with different time parameters to get as close as possible to the intermediate object. This leads to an optimization problem, where many time parameters need to be optimized across the whole surface structure. As a result, biologists could quantify the degree by which different parts of the animals differ from one species to another.

The main obstacle in applying shape morphing and shape models to such highly complex shapes is the amount of work necessary to create the models, in particular the point correspondence. Hence, we would like to investigate the automated methods for point correspondence for their suitability w.r.t. such highly complex biological objects.

References

[Ale03] ALEXA M.: Differential coordinates for local mesh morphing and deformation. *The Visual Computer 19*, 2 (2003), 105–114. 4

[BBK06] BRONSTEIN A. M., BRONSTEIN M. M., KIMMEL R.: Generalized multidimensional scaling: a framework for isometry-invariant partial surface matching. *Proceedings of the National Academy of Sciences 103*, 5 (2006), 1168–1172. 2

[BS08] BOTSCH M., SORKINE O.: On linear variational surface deformation methods. *IEEE Transactions on Visualization and Computer Graphics 14*, 1 (2008), 213–230. 2

[BT16] BAUM D., TITSCHACK J.: Cavity and pore segmentation in 3d images with ambient occlusion. In *EuroVis 2016 - Short Papers* (2016). doi:10.2312/eurovisshort.20161171. 2

[CCC*08] CIGNONI P., CALLIERI M., CORSINI M., DELLEPIANE M., GANOVELLI F., RANZUGLIA G.: Meshlab: an open-source mesh processing tool. In *Eurographics Italian chapter conference* (2008), vol. 2008, pp. 129–136. 2

[CSL*07] CARBON C.-C., STROBACH T., LANGTON S. R., HARSÁNYI G., LEDER H., KOVÁCS G.: Adaptation effects of highly familiar faces: Immediate and long lasting. *Memory & Cognition 35*, 8 (2007), 1966–1976. 1, 5

[FH05] FLOATER M. S., HORMANN K.: Surface parameterization: a tutorial and survey. In *Advances in Multiresolution for Geometric Modelling*. Springer, 2005, pp. 157–186. 2

[GJ*10] GUENNEBAUD G., JACOB B., ET AL.: Eigen v3. http://eigen.tuxfamily.org, 2010. 2

[KH13] KAZHDAN M., HOPPE H.: Screened poisson surface reconstruction. *ACM Transactions on Graphics (ToG) 32*, 3 (2013), 29. 2

[KS04] KRAEVOY V., SHEFFER A.: Cross-parameterization and compatible remeshing of 3d models. *ACM Transactions on Graphics (TOG) 23*, 3 (2004), 861–869. 2

[OMMG10] OVSJANIKOV M., MÉRIGOT Q., MÉMOLI F., GUIBAS L.: One point isometric matching with the heat kernel. In *Computer Graphics Forum* (2010), vol. 29, Wiley Online Library, pp. 1555–1564. 2

[RSB*15] REINDL A., STROBACH T., BECKER C., SCHOLTZ G., SCHUBERT T.: Crab or lobster? Mental principles underlying the categorization of crustaceans by biology experts and non-experts. *Zoologischer Anzeiger – A Journal of Comparative Zoology 256* (2015), 28–35. 1, 5

[SWH05] STALLING D., WESTERHOFF M., HEGE H.-C.: Amira: a highly interactive system for visual data analysis. In *The Visualization Handbook*. Elsevier, 2005, pp. 749–767. 2

[vKZHCO11] VAN KAICK O., ZHANG H., HAMARNEH G., COHEN-OR D.: A survey on shape correspondence. In *Computer Graphics Forum* (2011), vol. 30, Wiley Online Library, pp. 1681–1707. 2

[XZWB06] XU D., ZHANG H., WANG Q., BAO H.: Poisson shape interpolation. *Graphical Models 68*, 3 (2006), 268–281. 2

[ZLZ08] ZILSKE M., LAMECKER H., ZACHOW S.: Adaptive remeshing of non-manifold surfaces. In *Eurographics (Short Papers)* (2008), pp. 25–28. 2

[ZSH00] ZÖCKLER M., STALLING D., HEGE H.-C.: Fast and intuitive generation of geometric shape transitions. *The Visual Computer 16*, 5 (2000), 241–253. 2